A thermodynamic study on the effect of solute on the nucleation driving force, solid-liquid interfacial energy and grain refinement of Al alloys

Yijiang Xu, Dongdong Zhao, Yanjun Li*

Department of Materials Science and Engineering, Norwegian University of Science and Technology (NTNU), 7491 Trondheim, Norway

*Corresponding author, E-mail address: yanjun.li@ntnu.no

Abstract

Chemical composition is known to have significant effects on the grain refinement behavior of inoculated Al alloys during solidification. In this study, the influences of solute contents on the thermodynamic nucleation driving force and solid-liquid interfacial energy of binary Al alloys have been studied by CALPHAD method. The solute effect on the nucleation barrier and nucleation rate, thus on the grain refinement of Al alloys both with and without high potency nucleation particles, was analyzed based on the classical heterogeneous nucleation theory and free growth concept. Based on the classical heterogeneous nucleation theory, the calculation results reveal that Si has the effect of increasing the nucleation barrier of heterogeneous nucleation of grains and thus reduce the nucleation rate significantly. Alloying elements Cu and Mg have the effect of promoting heterogeneous nucleation and grain refinement. However, peritectic forming elements, e.g., Ti, Zr, V, have only negligible effects on the nucleation barrier. For solidification of Al alloys inoculated with high potency nucleation particles, the effect of nucleation driving force caused by different solute elements on the grain size of inoculated aluminum alloys has been quantitatively studied by a grain size prediction model for isothermal melt solidification. It is revealed that the solute dependent Gibbs-Thompson coefficients of Al-Cu, Al-Mg and Al-Si alloys have the influence of promoting the grain refinement by reducing the free growth undercooling.

Key words: Nucleation driving force, Solid-liquid interfacial energy, Solute effect, Grain refinement, Grain size

1. Introduction

It has been well recognized that solute elements, for instance, Ti, play a significant role in grain refinement of Al alloys during casting of aluminum since the 1930s [1]. As stated by Cibula [2] in 1949, there are mainly two kinds of grain refinement mechanisms: the first is the restriction of crystal growth by concentration gradients in the liquid around solidifying dendrites and thus allowed the interior of the casting to undercool and therefore new crystallites could form, e.g., Cu has such an effect; the second is formation of nuclei, such as intermetallic compound or carbide particles, which facilitate nucleation, e.g., addition of Ti, B, Nb or Zr has such an effect.

Based on the constitutional supercooling concept for equiaxed formation proposed by Winegard and Chalmers [3], Tarshis et al. [4] found that the addition of solute led to substantial grain refinement in a variety of Ni- and Al-based alloys and proposed the supercooling parameter P, defined below, to correlate with the grain size.

$$P = \frac{mC_0(k-1)}{k}, \quad (1)$$

where C_0 is the bulk melt solute content, m is the liquidus slope and k is the partition coefficient. The grain structure and grain size showed a strong dependence on this parameter for dilute binary alloys both with and without addition of potent inoculation particles [4-6]. This parameter represents the equilibrium melting temperature distribution ahead of an advancing solid/liquid interface under steady state [4, 7], which numerically equals to the solidification range [4, 5] for dilute alloys where the liquidus and solidus lines are straight. However, if the solute content C_0 is larger than the maximum solubility C_m, as suggested by Xu et al. [8], P should be modified as $m(C_0 - C_E)$, since maximum solute concentration at the S/L interface changes from C_0/k to eutectic composition C_E when $C_0 > C_m$. Such a new parameter P^* or solidification interval ΔT was supposed to correlate well with the experimentally measured grain size [8] in Al-Cu alloys without inoculation except for the grain size minimum point (~10.5 wt.% in their experiment rather than C_m, 5.65wt.%). However, different researchers reported different experimental results in Al-Cu [5, 9] alloys, where grain size monotonically decreases as copper content increases. In addition, it is well known that the grain size evolution of Al-Si [9-14] alloys (without inoculation) as a function of Si content shows a 'V' type shape with a transition point at 3wt.% Si, which is far from the maximum solubility or maximum ΔT point. Also, the experimental minimum grain size point also varies when different solidification conditions (temperature gradient and cooling rates) are used, indicating that other parameters than constitutional parameter or solidification interval could also influence the final grain size. The V-shape grain size evolution as a function of solute content has been ascribed to dendrite growth morphology change [11, 15] and the nucleation activation energy increase with further increasing Si contents after the bottom point of 'V' type curve [13]. However, up to now, it is still short of rigorous theoretical investigation and compellent mechanism.

Another parameter to predict the relative grain size was proposed by Moriceau [16], originally called alloy system dependent parameter X [17], and the inverse of this parameter $1/X$ was taken as an inhibitor to growth. Similar to the Cibula [2]'s theory, the restriction of grain growth at a high value of $1/X$, reduces the latent heat generation and gives longer time for further nucleation to occur. This leads to the nucleation of more grains and thus a smaller final grain size. The parameter $1/X$ was termed as the growth restriction factor by Johnsson [18, 19], based on the suggestions that the growth velocity of dendrite tip is inversely proportional to the factor $mC_0(k-1)$ [20, 21]. Later, the growth restriction factor has also been termed as GRF [22] and Q [23], as described by Eq.(2).

$$\frac{1}{X} = Q = mC_0(k-1) \quad (2)$$

It has been verified experimentally that grain size decreases with increasing Q values for inoculated low solute concentration Al alloys [19, 23-25]. But, as reported by Hutt et al. [9] and Xu et al. [8], the relationship between the grain size and Q is not monotonic in the whole range of hypoeutectic Al-Si and Al-Cu alloys.

Since growth restriction factor and constitutional supercooling have indirect influences on the nucleation process, approaches were also proposed to directly evaluate the effect of solute elements on the nucleation barrier and nucleation rate of grains. Based on the regular solution assumption, Youdelis [26] calculated the nucleation entropy for binary alloys and found out that for binary eutectic systems, the absolute value of the molar entropy of nucleation increases progressively with solute concentration up to the eutectic limit. It showed that the nucleation rate and grain refinement should increase with solute concentration. Yang and

Youdelis [27, 28] calculated the nucleation entropy for Al-Ti alloys and an increase of nucleation entropy with Ti content up to 0.15wt.% was predicted. Later, Yao et al.[29] reported composition-dependent nucleation driving force ΔS_f in Al-Si and Al-Cu alloys based on Youdelis's model [26] but with many simplifications. It was shown that ΔS_f decreases steadily with Si content but remains almost constant with Cu content, which means that Si could reduce the barrier for nucleation to enhance the possibility of nucleation but Cu has no significant effect. Such calculation results are not identical to the Youdelis [26]'s original prediction results for Al-Cu alloys and the experimental results of Al-Si alloys reported in the literature [9, 13, 14]. In a recent work, Wang et al.[30] studied the effect of solute on the thermodynamic driving force for solidification (including nucleation and growth) in Al alloys by CALPHAD method. It reveals that addition of solute reduces the driving force for solidification at a given undercooling. For a constant Q value, the solidification driving force is reduced more substantially when adding eutectic forming solutes than peritectic forming elements. However, the grain refinement is a result of competition between nucleation and grain growth, where faster nucleation while lower growth rate are beneficial to grain refinement. Hence, the driving force of solidification, as a combined process of both nucleation and grain growth, is difficult to be linked directly to the grain refinement effect and the final grain size.

Nevertheless, in addition to the growth restriction effect, solute elements can also influence the grain refinement behavior of Al alloys by affecting the nucleation entropy ΔS_N and the volumetric Gibbs free energy difference between the liquid and solid phase ΔG_v. According to the classical nucleation theory, the solid-liquid interfacial energy σ_{SL} also contributes to the nucleation barrier. However, most of the previous theoretical investigations have been based on a constant σ_{SL} assumption, without considering the solute effect on it. Therefore, the present work is aimed at a theoretical investigation on the effect of solute additions on the nucleation driving force, in terms of both $\sigma_{SL}$and ΔG_v by using the CALPHAD approach with sophisticated Gibbs free energy functions. CALPHAD has been widely applied in solidification [31-33], additive manufacturing [34], solid-state phase transformation [35, 36] and materials design [37], e.g., calculating growth restriction factor Q of multicomponent alloys [38], coupling with phase-field model to simulate microstructure evolution [39, 40], phase evolution prediction during heat treatment and precipitation modelling[35, 36, 41, 42]. Based on the calculation results, the effects of different solute elements on the grain refinement was analysed and discussed for binary Al alloys with and without adding high potency inoculation particles.

2. Thermodynamic modelling

According to the classical nucleation theory, the nucleation rate for heterogeneous nucleation can be calculated by [43] :

$$I = I_0 \cdot \exp\left(-\frac{\Delta G_n^0}{k_B T}\right) = v_0 p_c n_p \cdot \exp\left(-\frac{16\pi \cdot f_\theta}{3k_B}\frac{{\sigma_{SL}}^3}{(\Delta G_v)^2 \cdot T}\right), \quad (3)$$

where I_0 is a prefactor determined by the atomic vibration frequency v_0, the probability of capturing an atom at the surface of solid phase p_c and the density of particles in the melt n_p, k_B is Boltzmann constant, T is the melt temperature, ΔG_n^0 is the nucleation barrier of heterogeneous nucleation, which is a function of the contact angle factor f_θ, σ_{SL} and ΔG_v. It

is obvious that the nucleation rate is mainly controlled by the exponential term Ψ in the bracket ($\Psi = -\frac{16\pi \cdot f_\theta}{3k_B} \frac{{\sigma_{SL}}^3}{(\Delta G_v)^2 \cdot T}$).

The Gibbs free energy difference for nucleation ΔG_v in alloys is calculated based on the suggestion by Thompson and Spaepen [44]. As shown in Fig. 1(a), for a liquid with a concentration of c_L, at liquidus temperature T_L, the equilibrium concentration of solid phase is $c_{S,eq}$. In the undercooled liquid, the composition of the nucleated solid crystal, c_S, should be determined by maximizing the Gibbs free energy change for the formation of per mole nucleus, ΔG. The maximum of ΔG is obtained when the chemical potential change of component A and B, $\Delta\mu_A$ and $\Delta\mu_B$ are equal to each other. And therefore, the composition c_S is found by drawing a tangent line to the free energy curve of the solid G^S, which is parallel to the tangent line of the free energy curve of liquid G^L at c_L, as depicted in Fig. 1(b), so that

$$\Delta G = \Delta\mu_A = \Delta\mu_B \tag{4}$$

$$\left(\frac{\partial G^L}{\partial c_L}\right)_{c_L} = \left(\frac{\partial G^S}{\partial c_S}\right)_{c_S} \tag{5}$$

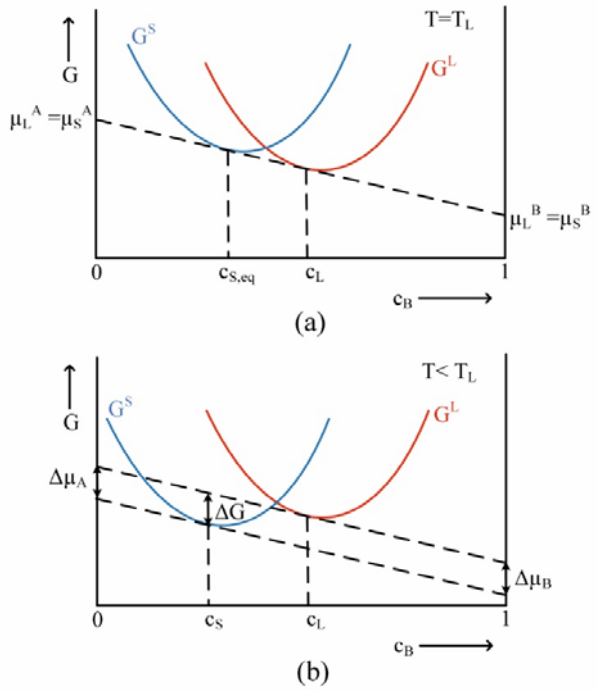

Fig. 1. Schematic mole Gibbs free energy-composition diagram: (a) at the liquidus temperature, T_L, (b) below T_L, at arbitrary nucleation temperature. The free energy change ΔG associated with forming a small nucleus of composition c_S in the liquid of composition c_L is obtained by the parallel tangent construction [44, 45]. Adapted from [44] with additional data from [45].

Therefore, given the composition and temperature dependence of the liquid and solid free energies, one can calculate the solid nucleus composition and the free energy for the formation of the nucleus as a function of initial liquid composition c_L and undercooling $\Delta T =$

$T_L - T$. For an accurate calculation of ΔG, the Gibbs free energy for α-Al solid solution (G^S) and liquid phases (G^L) are described by the substitutional solution model as follows:

$$G^{\phi} = \sum_i c_i \cdot G_i^{0,\phi} + RT \sum_i c_i \cdot lnc_i + \sum_{i,j>1} c_i \cdot c_j \cdot \sum_v L_{i,j}^{v,\phi} (c_i - c_j)^v, \quad (6)$$

where ϕ is the state of phase (S represents solid and L represents liquid), c_i (c_j) represents the mole fraction of element i (j), with i (j) =Al, Cu, Mg, Si, Ti, Zr, V; R is the gas constant (R = 8.3143 J mol^{-1}K^{-1}) and $L_{i,j}^{v,\phi}$ is the Redlich-Kister parameter representing the interaction between elements i and j, the value of which can be obtained from COST 507 database [46]. Meanwhile, the temperature-dependent Gibbs free energy function $G_i^{0,\phi}$ for pure element i in any phase is available and can be taken from SGTE (Scientific Group Thermodata Europe) tabulated data by Dinsdale [47].

After solving Eq. (5), c_S is obtained, then ΔG can be calculated by [48]:

$$\Delta G = \mu_A^L - \mu_A^S = G^L - c_L \frac{\partial G^L}{\partial c_L} - \left(G^S - c_S \frac{\partial G^S}{\partial c_S} \right). \quad (7)$$

Eq. (7) gives Gibbs free energy per mole (J/mol), but in the classical nucleation theory, Gibbs free energy per unit volume (J/cm^3 or J/m^3) of crystal is needed, so

$$\Delta G_v = \Delta G / V_{s,m}, \quad (8)$$

where $V_{s,m}$ is the average molar volume of the solid, and herein is assumed to vary linearly between the molar volumes of the pure solid systems V_m^A and V_m^B [44, 49]:

$$V_{s,m} = c_s^A V_m^A + (1 - c_s^A) V_m^B. \quad (9)$$

The temperature dependence of molar volume of the pure element can be found in Ref. [50].

The composition and temperature dependence of σ_{SL} is calculated by the thermodynamic model proposed by Granasy and Tegze [51, 52], considering both the melting enthalpy and melting entropy:

$$\sigma_{SL} = \alpha \frac{\Delta H_{f,m} + T_m \Delta S_{f,m}}{2 \cdot \left(N_A \cdot {V_{s,m}}^2 \right)^{\frac{1}{3}}}, \quad (10)$$

where α is the dimensionless interfacial energy and $\alpha = 0.561$ [53] for FCC Al, T is the temperature, N_A is the Avogadro's number, and $\Delta S_{f,m}$ is the molar entropy of fusion for alloys. $\Delta S_{f,m}$ can be determined by calculating the entropy difference between the nucleated solid and liquid metal, using available Gibbs free energy function directly without regular solution assumption:

$$\Delta S_{f,m} = S_l(T, c_l) - S_s(T, c_s) = \left(\frac{\partial G_l}{\partial T} \right)_{C_l} - \left(\frac{\partial G_s}{\partial T} \right)_{C_s} = -\Delta S_N \quad (11)$$

ΔS_N is the nucleation entropy. Besides, $\Delta H_{f,m}$ is the molar enthalpy of fusion of the solid layer, and it can be calculated by the following equation:

$$\begin{aligned} \Delta H_{f,m} &= H_l(T, c_l) - H_s(T, c_s) \\ &= \left(G_l(T, c_l) + T \left(\frac{\partial G_l}{\partial T} \right)_{C_l} \right) - \left(G_s(T, c_s) + T \left(\frac{\partial G_s}{\partial T} \right)_{C_s} \right). \end{aligned} \quad (12)$$

In the present work, commercial software Thermo-Calc [54] has been used to calculate the liquidus temperature of the binary Al alloys and the equilibrium concentration of solid phase $c_{s,eq}$ based on equilibrium condition (Fig. 1a). The calculation was made based on the COST 507 thermodynamic database [46]. Further thermodynamic calculation (solving Eq.(4)-(12)) is realized by Matlab [55] programming using the same database.

3. Results and discussion

3.1. Influence of solute content on heterogeneous nucleation of uninoculated aluminum alloys

The ΔG_v and σ_{SL} at different undercoolings ΔT as a function of solute content of different Al alloys were calculated firstly. According to the classical theory for heterogeneous nucleation, the critical nucleation activation energy or nucleation barrier ΔG_n^0 is $(\frac{16\pi}{3}) \cdot (\frac{{\sigma_{SL}}^3}{(\Delta G_v)^2}) \cdot f_\theta$. The contact angle θ and thus f_θ are influenced by many factors, such as substrate particle type and property, solid-liquid interfacial energy, etc. It is generally difficult to determine the values of θ. Therefore, f_θ is assumed as the same but independent of solute contents in this work (the same assumption as in Ref. [29, 56]). Then, the relative value of ΔG_n^0 of Al alloys to pure Al, $\frac{\Delta G_{n,Al-X}^0}{\Delta G_{n,Al}^0}$, were also calculated. A value of $\frac{\Delta G_{n,Al-X}^0}{\Delta G_{n,Al}^0} > 1$ indicates that the nucleation barrier increases with increasing solute concentration of the alloys, namely, a higher concentration will reduce the nucleation driving force. On the other hand, when $\frac{\Delta G_{n,Al-X}^0}{\Delta G_{n,Al}^0} < 1$, an increased composition can decrease the nucleation barrier and enhance the possibility of nucleation in the undercooled liquid. It should be noted that since the liquidus temperature of the alloy T_l varies with the solute species and concentration, under the same undercooling $\Delta T = T_l - T$, the melt temperature T may also have a contribution to the nucleation rate, as indicated by Eq. (3). Therefore, the relative value of the exponential term to pure Al, $\frac{\Psi_{Al-X}}{\Psi_{Al}}$ could be obtained as well.

After calculating these parameters at different undercoolings, Al-Cu binary alloy was taken as an example to show the undercooling effect (Fig. 2). It is found that ΔG_v increases with undercooling ΔT while other parameters are not influenced much by ΔT. By further dividing ΔG_v with ΔT, it can be seen that $-\Delta G_v/\Delta T$ at different undercoolings are almost the same (Fig. 2a). Thus, the calculation results at $\Delta T = 1\ K$ are representative and are adopted in this section.

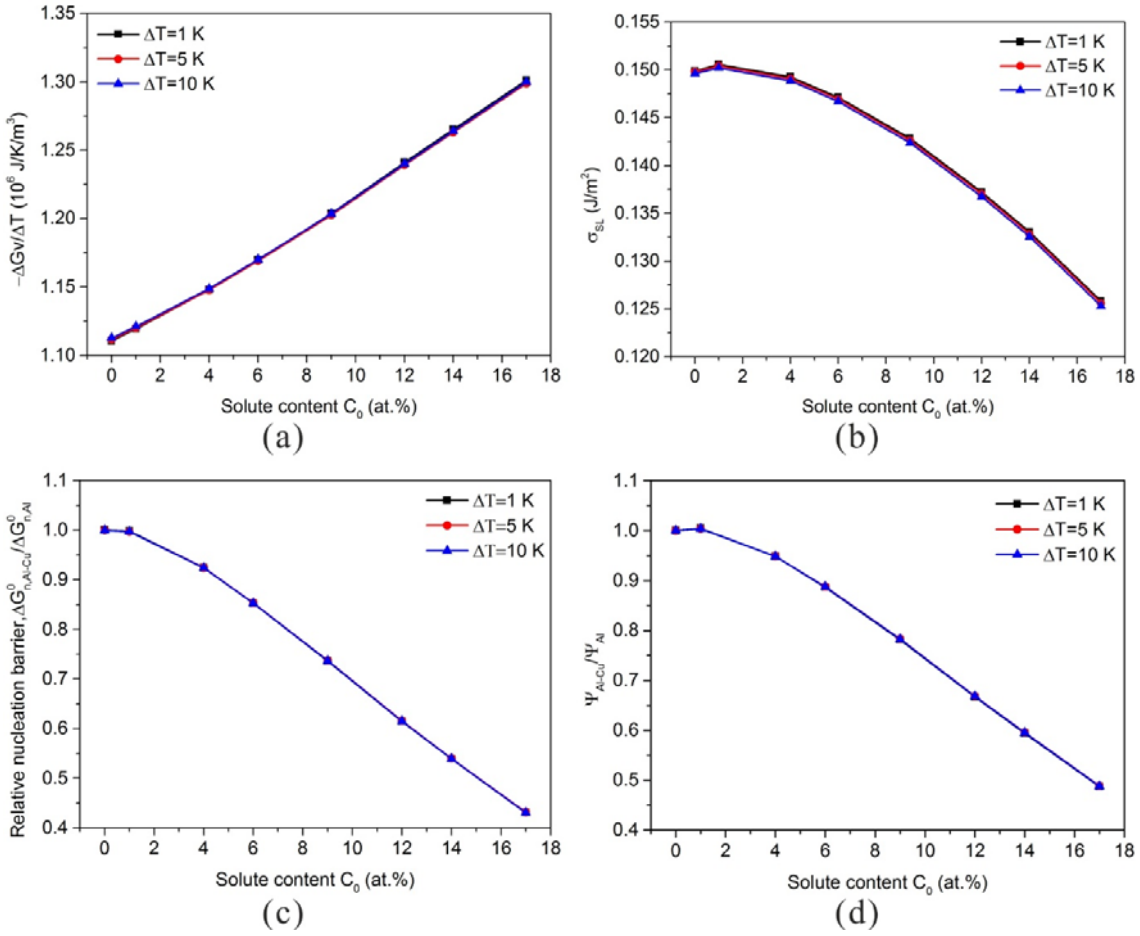

Fig. 2. Calculated Gibbs free energy change per undercooling $\Delta G_v/\Delta T$, solid-liquid interfacial energy σ_{SL}, relative critical nucleation energy and relative Ψ to pure Al, $\frac{\Delta G^0_{n,Al-X}}{\Delta G^0_{n,Al}}$ and $\frac{\Psi_{Al-X}}{\Psi_{Al}}$, with different solute contents (at.%) at three different undercoolings $\Delta T = 1, 5, 10\ K$ for hypoeutectic Al-Cu alloys.

3.1.1. Influence of eutectic forming elements

The calculated $-\Delta G_v$, σ_{SL}, $\frac{\Delta G^0_{n,Al-X}}{\Delta G^0_{n,Al}}$, $\frac{\Psi_{Al-X}}{\Psi_{Al}}$, of hypoeutectic Al-Cu, Al-Mg and Al-Si alloys with different solute contents (at.%) at an undercooling of $\Delta T = 1\ K$ are shown in Fig. 3. The absolute value of ΔG_v increases with solute content for Al-Cu and Al-Si alloys, but shows an opposite trend for Al-Mg alloys. The present calculation results for Al-Cu is different from the calculation results by Yao et al. [29], who used ideal solution model to calculate nucleation entropy for alloys. According to present calculation, Cu solute also increase the driving force for nucleation. Also different from the calculation results by Wang et al.[30], which showed a reduction of solidification driving force ΔG_v with increasing the addition level of solutes, either eutectic forming or peretectic forming elements. The present work shows that the ΔG_v can both increase or decrease with solute content, which is alloy dependent, for example, Al-Cu and Al-Mg alloys show opposite trends at a given undercooling.

Besides the nucleation driving force ΔG_v, the solid-liquid interfacial energy σ_{sl} plays an important role in nucleation, since it is one of the major nucleation barriers. As can be seen from Fig. 3b, the solid-liquid interfacial energy σ_{SL} of Al alloy decreases with the amount of Cu and Mg solute, but increases with Si solute content, showing the same trend with the results calculated by Lippmann et al. [52] using FactSage [57]. As already discussed by the authors [52], a reliable evaluation of the concentration dependence of solid/liquid interfacial energies of alloys is difficult since the available experimental data of Al alloys are very limited. Nevertheless, the calculation can reproduce qualitatively the trends shown by experimental data [52].

From Fig. 3c and 3d, it can be seen that adding Si to pure Al would increase the critical nucleation energy and thus reduce the nucleation rate significantly. It is consistent with the experimental results [9-14] that the grain size of non-inoculated Al-Si alloys increases with increasing Si content when Si content is larger than about 3 wt.%. The decrease of grain size with increasing Si content in the low Si content alloys (< 3 wt.%.) should be attributed to the grain growth restriction effect, which may play a more important role than increasing critical nucleation energy. For other two eutectic forming elements, Cu and Mg, both would promote nucleation rate based on present thermodynamic calculation results. Together with the increasing of the growth restriction factor Q, both Cu and Mg would promote grain refinement in Al-Cu and Al-Mg alloys. Such kind of prediction is supported by the experimental results reported by Hutt and StJohn [9], Yang et al. [58] for Al-Cu alloys and Birol [59] for Al-Mg alloys until the near eutectic point (~30wt.%). Different from the above results, Xu et al. [8] found that the grain size first decreases and then increases with Cu content at higher concentration (> 10wt.% Cu). They argued that dendrite fragmentation is mainly responsible for the formation of equiaxed grains in high-purity Al-Cu alloys rather than heterogeneous nucleation. Such dendrite fragmentation is influenced by the maximum constitutional undercooling or the solidification interval ΔT. Since pouring method, instead of TP-1 type casting, was used to cast samples in their experiments, dendrite fragmentation was more pronounced in their solidification experiments. Nevertheless, as summarized by Spittle [60], in reality, it is likely that several mechanisms may be operative in a particular casting situation. For instance, for the normal casting with pouring, big bang nucleation at the mold wall, dendrites fragmentation, and heterogeneous nucleation would be operative at the same time. However, for TP-1 type solidification, heterogeneous nucleation dominates. In other words, constitutional undercooling parameter P, solidification interval ΔT, growth restriction factor Q, and heterogeneous nucleation rate have a combination effect on the equiaxed grains formation and thus the final grain size. This is the reason why different trends for grain size evolution as a function of solute contents were observed under different solidification conditions for the same alloy system.

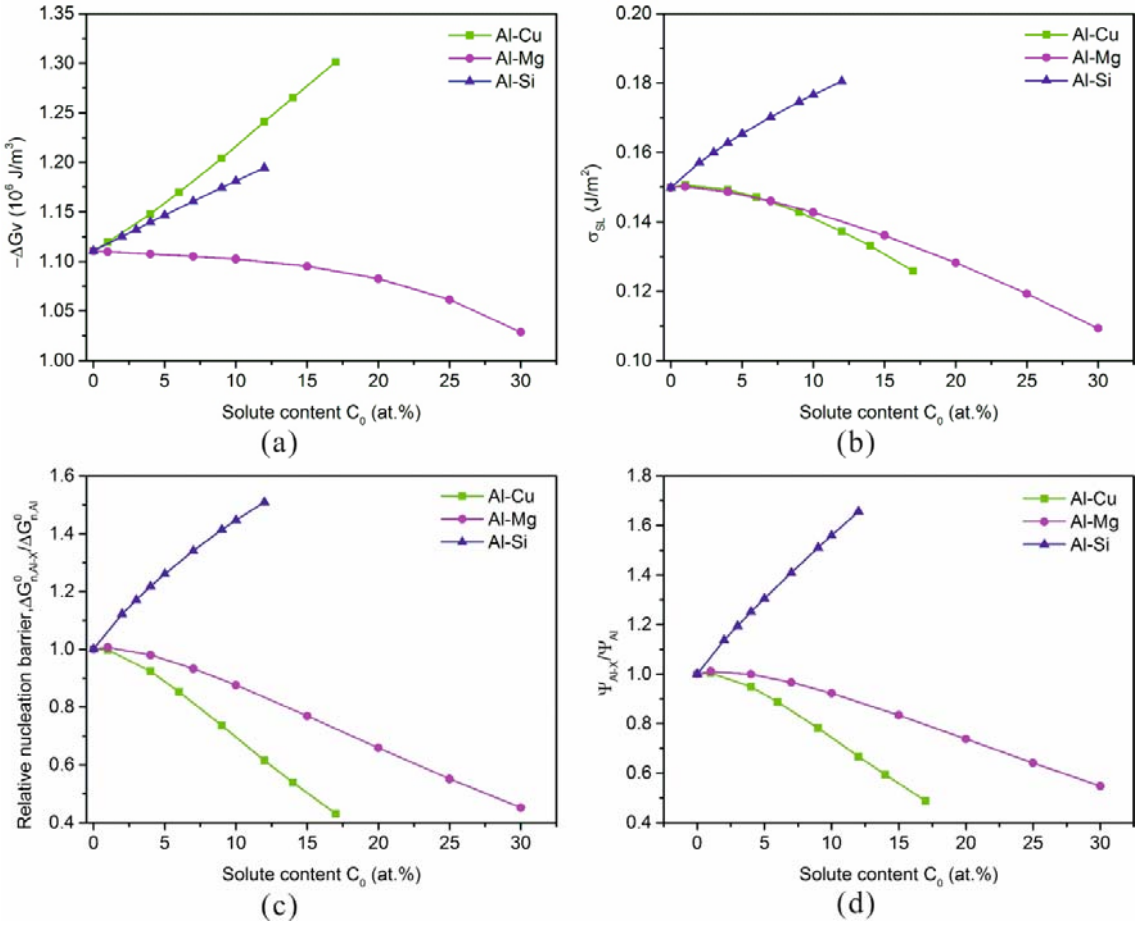

Fig. 3. Calculated Gibbs free energy change ΔG_v, solid-liquid interfacial energy σ_{SL}, relative critical nucleation energy and relative Ψ to pure Al, $\frac{\Delta G^0_{n,Al-X}}{\Delta G^0_{n,Al}}$ and $\frac{\Psi_{Al-X}}{\Psi_{Al}}$, with different solute contents (at.%) at undercooling $\Delta T = 1\ K$ for hypoeutectic Al-Cu, Al-Mg and Al-Si alloys.

3.1.2. Influence of peritectic forming elements

The calculated $-\Delta G_v$, σ_{SL}, $\frac{\Delta G^0_{n,Al-X}}{\Delta G^0_{n,Al}}$, $\frac{\Psi_{Al-X}}{\Psi_{Al}}$ as a function of solute contents (at.%) at an undercooling of $\Delta T = 1\ K$ for hypoperitectic Al-Ti, Al-Zr and Al-V alloys are shown in Fig. 4. As can be seen from Fig. 3a, for the three peritectic alloy systems investigated, Ti can increase the nucleation driving force (ΔG_v); However, Zr and V both reduce the nucleation driving force. Regarding the effect of Ti, the present result is consistent with the prediction by Yang and Youdelis [27]. This result is different from the solidification driving force results calculated by Wang et al.[30], which always decreases with increasing the solute contents. Fig. 3b shows the calculated solid-liquid interfacial energy σ_{sl} of different alloys as a function of solute contents. All of three peritectic forming elements, Ti, Zr and V, would increase the value of σ_{sl} slightly.

From Fig. 4c and 4d, it can be seen that the present three peritectic forming elements tend to increase the nucleation barrier slightly and may reduce the heterogeneous nucleation rate. If no Al-V, Al-Ti or Al-Zr intermetallic particles form in the melt, the final grain size of the alloys will be controlled by the competition between growth restriction, constitutional

undercooling and thermodynamic nucleation barrier. According to the experimental results reported by Wang et al.[61], below the peritectic composition, Zr and V have little or no effect on the grain refinement of commercial-purity Al, but Ti significantly refines the grain size. Our calculation results support the experimental results for Al-Zr and Al-V systems but not for Al-Ti alloys. According to present thermodynamic calculation, it is clear that adding Ti solute itself can neither increase the nucleation driving force significantly nor reduce the nucleation barrier. The strong grain refinement effect of Ti solute below the peritectic point should be attributed to other reasons. Cibula et al. [2] firstly proposed the TiC hypothesis, where Ti reacted with C in aluminium melt to form potent TiC particles, acting as the nucleation substrate of aluminum grains. As reviewed by Guzowski et al. [62], some researchers believed that $TiAl_3$ acted as the nucleation substrate. However, no direct observations have been reported in the literature. Easton and StJohn et al. [63, 64] suggested the strong segregation power and the extremely high growth restriction factor of Ti is crucial for the grain refinement. In a recent work, Chen et al.[65, 66] reported that a large number of fine grains which are in a twin, or near-twin, relationship with their nearest neighbors in the as-cast Al-0.1%Ti and Al-5%Cu-0.1%Ti alloys. This result is similar to that in [67, 68]. Therefore, the authors speculated that Ti-containing quasicrystals may have formed in the melt and worked as potential nucleation sites in the alloys. Thus, the exact mechanism is still an unsolved question and more studies are necessary.

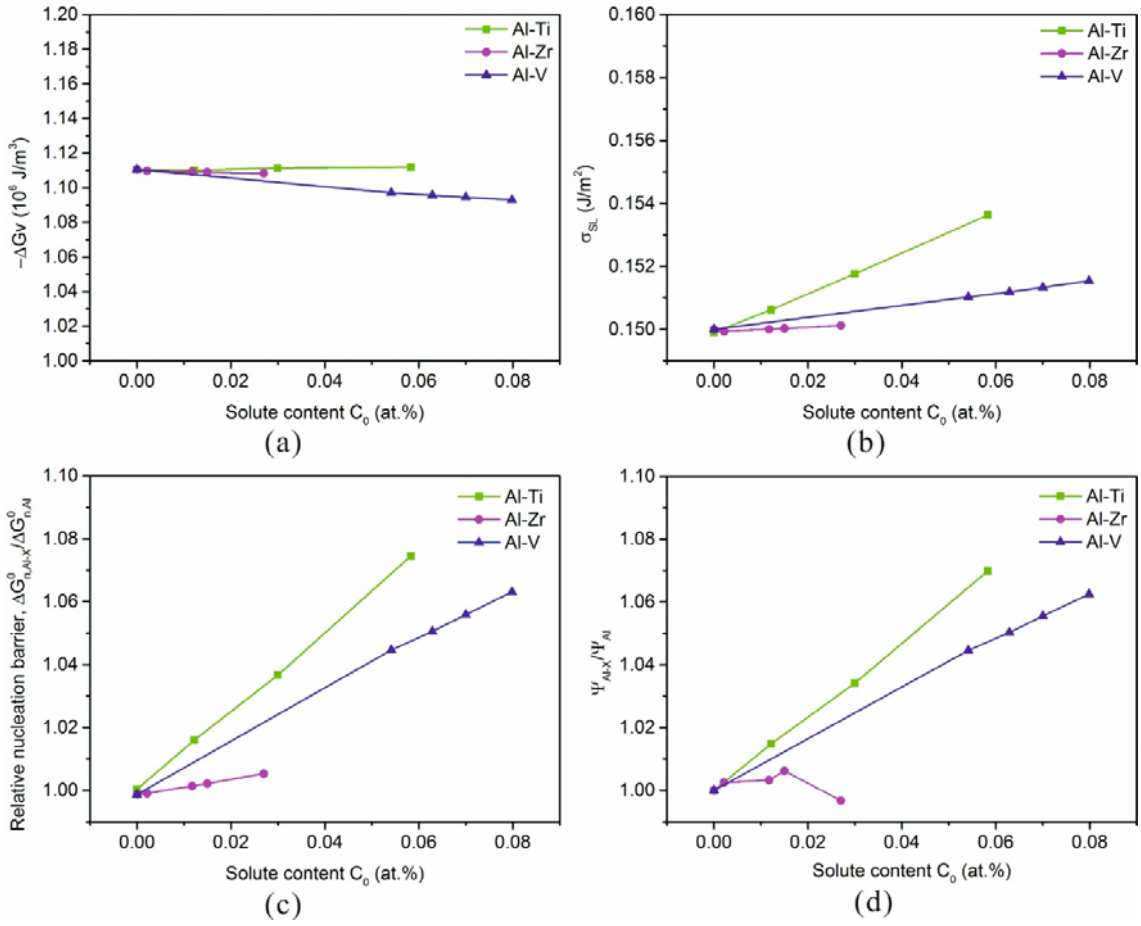

Fig. 4. Calculated Gibbs free energy change ΔG_v, solid-liquid interfacial energy σ_{SL}, relative critical nucleation energy and relative Ψ to pure Al, $\frac{\Delta G^0_{n,Al-X}}{\Delta G^0_{n,Al}}$ and $\frac{\Psi_{Al-X}}{\Psi_{Al}}$, with different solute contents (at.%) at undercooling $\Delta T = 1\ K$ for hypoperitectic Al-Ti, Al-Zr and Al-V alloys.

3.2. Influence of solute content on heterogeneous nucleation of inoculated aluminum alloys

The heterogeneous nucleation of α-Al grains in Al alloys inoculated by high potency Al-Ti-B or Al-Ti-C master alloys is a deterministic process [23, 69]. The heterogeneous nucleation on inoculation particles is instantaneous, and the rate-limiting step for the successful formation of α-Al grain is the initiation of free growth, which occurs at the geometrically dependent undercooling ΔT_{fg}, given by

$$\Delta T_{fg} = \frac{4\Gamma}{d} = \frac{4\sigma_{SL}}{\Delta S_v d} \tag{13}$$

where σ_{SL} is the solid–liquid interfacial energy, ΔS_v is the entropy of fusion per unit volume and Γ is the Gibbs-Thomson coefficient. Hence, the ratio between σ_{SL} and ΔS_v (Γ) determines the undercooling needed for the onset of free growth of given inoculant particles. In most of the previous grain size prediction models [31, 70-76], the σ_{SL} and ΔS_v data of pure Al is used for Al alloys. Some researchers [77] chose different Γ values for different alloy system, but neglected the concentration dependence of the solute elements. In the present work, the influence of solute elements and contents on Γ was calculated by the thermodynamic approach combined with the solid-liquid interface model. It should be noted that the undercooling has negligible influences on ΔS_v, σ_{SL} and Γ. Therefore, only the calculation results at liquidus temperature are presented here.

3.2.1. Influence of eutectic forming elements

The calculated ΔS_v as a function of solute content C_0, for three eutectic binary Al alloys, Al-Cu, Al-Mg and Al-Si alloys, at respective liquidus temperature are shown in Fig. 5a. It can be seen that the value of ΔS_v for eutectic alloy systems are larger than that for pure Al. It is interesting to note that, for Al-Mg alloys, ΔS_v curve shows a parabolic shape, namely, it firstly increases and then decreases with the solute content. This is different from the calculation result by Youdelis [26], which showed a monotonic increase of ΔS_v with Mg content. It should be noted that the calculation by Youdelis [26] is based on the regular solution assumption but no such assumption is used in the present calculation. However, the reason for such a parabolic evolution of ΔS_v as a function of Mg content needs further study. By comparing ΔS_v to the Gibbs free energy change curve shown in Fig. 3a, it can be seen that $\Delta G_v \neq \Delta S_v \cdot \Delta T$ for alloys. In terms of solid-liquid interfacial energy at respective liquidus temperature, it is just nearly the same as the previous results at 1 K undercooling shown in section 3.1.

The relative Gibbs-Thomson coefficient defined as the ratio between Γ_{Al-X} of alloy and Γ_{Al} of pure Al, $\frac{\Gamma_{Al-X}}{\Gamma_{Al}}$, is plotted in Fig. 5b. As shown in Fig. 5b, through adding eutectic-forming solute elements like Cu, Mg and Si, the relative Gibbs-Thomson coefficient is always smaller than 1 and can decrease to 0.63 as solute content is approaching the eutectic composition. This indicates that addition of eutectic-forming solute elements can reduce Γ and therefore the free growth undercooling ΔT_{fg}. According to the free growth model, a smaller value of

ΔT_{fg} means the nucleation of α-Al grains on the same sized inoculant particles is easier. In addition, the growth restriction factor Q increases monotonically with the solute content. Therefore, for the solidification of Al melt inoculated with high potency grain refiners, eutectic-forming solute elements can simultaneously promote nucleation and suppress grain growth.

It is interesting to note that solute Si has different effects on nucleation of grains for non-inoculated and inoculated Al-Si alloys. It inhibits heterogeneous nucleation of grains for the former case (Fig. 3c), while promotes the nucleation for the latter case (Fig. 5b). The reason for the different influences can be explained as follows. For non-inoculated alloys, the critical nucleation barrier increases and therefore the nucleation rate decreases with increasing Si content in the alloy. However, for the inoculated alloys, according to the athermal nucleation theory by Greer et al, the formation rate of spherical caps of nuclei on inoculant particles is not controlled by the nucleation barrier but rather the free growth undercooling, which is determined by Gibbs-Thompson coefficient Γ and the diameter of inoculant particles. A decrease of Γ with increasing Si content means that the free growth of grains is promoted. Such calculation results are supported by many experimental results reported in the literature. For aluminium alloys containing low content of Si (no poisoning of TiB_2 or TiC inoculant particles by solute Si), it is found that adding Si solute promotes grain refinement [14]. For Al-B master alloy inoculated Al-Si alloys, the grain refinement effect is also shown to increase with increasing Si content [14, 78].

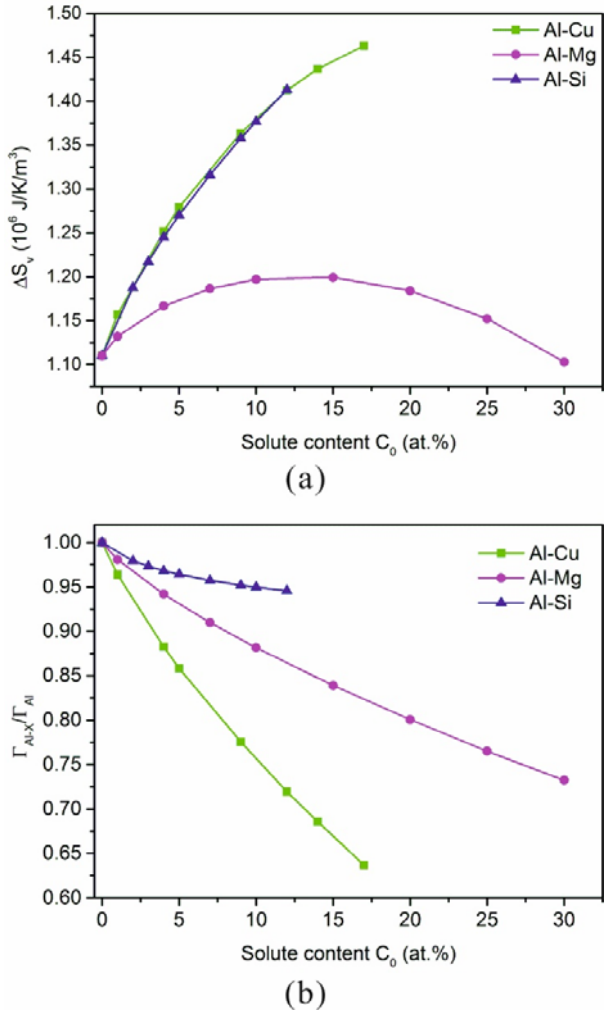

Fig. 5. Calculated entropy of fusion per unit volume ΔS_v, and relative Gibbs-Thompson coefficient Γ to pure Al, $\frac{\Gamma_{Al-X}}{\Gamma_{Al}}$, with different solute contents (at.%) at respective liquidus temperature for hypoeutectic Al-Cu, Al-Mg and Al-Si alloys.

3.2.2. Influence of peritectic forming elements

The calculated ΔS_v and relative Gibbs-Thompson coefficient Γ to pure Al, $\frac{\Gamma_{Al-X}}{\Gamma_{Al}}$, as a function of solute content C_0, for three peritectic binary Al alloys, Al-Ti, Al-Zr and Al-V, at respective liquidus temperature are shown in Fig. 6. As can be seen, the value of ΔS_v for the peritectic alloy systems decreases slowly with increasing alloying element contents. Since these elements slightly increase σ_{SL} of the alloys, an addition of these elements only slightly increases the Γ values of the alloys (Fig. 6b). As the maximum increase of Γ is only about 3%, the effect of addition of the three elements on the free growth undercooling ΔT_{fg} probably can be neglected. Therefore, in the inoculated Al alloys, peritectic-forming solute elements below peritectic composition should not have a direct influence on the heterogeneous nucleation but mainly contribute to the growth restriction effect (see further verification in Section 3.2.3), which also benefits the grain refinement.

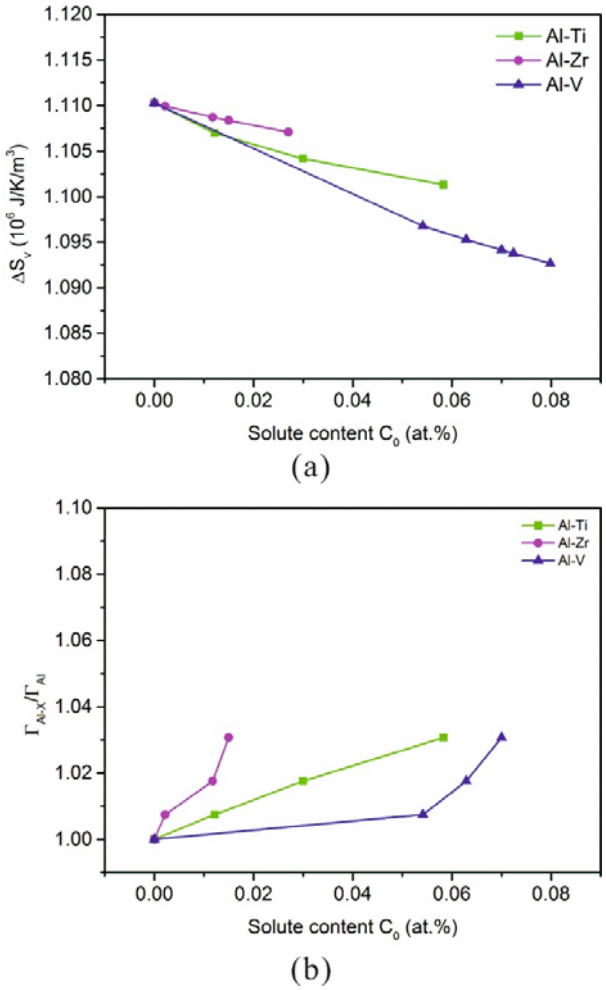

Fig. 6. Calculated entropy of fusion per unit volume ΔS_v, and relative Gibbs-Thompson coefficient Γ to pure Al, $\frac{\Gamma_{Al-X}}{\Gamma_{Al}}$, with different solute contents (at.%) at respective liquidus temperature for hypoperitectic Al-Ti, Al-Zr and Al-V alloys.

3.2.3 Quantitative investigation of solute dependent Γ on grain size

To examine the effect of Gibbs-Thomson coefficient Γ on the final grain size of inoculated aluminium alloys, quantitative grain size prediction was carried out by using a recently proposed grain size prediction model [76, 79]. In the model, Γ is set as constant or solute concentration dependent to compare the solute effect on grain nucleation. The parameters for pure Al were used as reference: $\sigma_{SL} = 0.15$ J/m^2, $\Delta S_v = 1.1 * 10^6$ J/k/m^3 and thus $\Gamma_{Al} = 1.36\, K \cdot m$.

For eutectic system, Al-Cu alloys with different Cu content inoculated by 0.1 wt.% Al-5Ti-1B, with constant cooling rate of 1 K/s during isothermal solidification conditions were used as calculation cases. The predicted grain sizes are shown in Fig. 7a. It can be seen that, as Cu content increases, the predicted grain size decreases significantly even when the Gibbs-Thomson coefficient Γ is constant, which is a result of grain growth restriction effect. When a composition dependent Γ is included in the numerical model, a smaller value of grain size is obtained. It confirms that Cu solute has the influence of enhancing the grain nucleation by reducing the interfacial energy σ_{SL}, and increasing entropy of fusion ΔS_v.

For peritectic system, the solidification cases of Al-Ti alloys with different Ti contents inoculated by 0.03% TiB_2, with initial cooling rate of 0.8 K/s solidified in the heated cast iron mould [63, 64] were simulated based on recalescence nucleation stifling mechanism. The simulation results are compared with the experimental results, as shown in Fig. 7b. As can be seen, the prediction results based on constant Γ are nearly coincident with those based on Ti dependent Γ, which confirms the solute elements almost have no influence on free growth undercooling and grain refinement behaviour. Besides, the prediction results are in a good agreement with the experimental measurements, and both show that the grain size decreases with increasing Ti solute content. According to the present model mechanism, it can be concluded that this grain refinement of Ti solute should be due to the growth restriction effect (Q increases with solute content, and Q=22 K at 0.15 wt.%Ti).

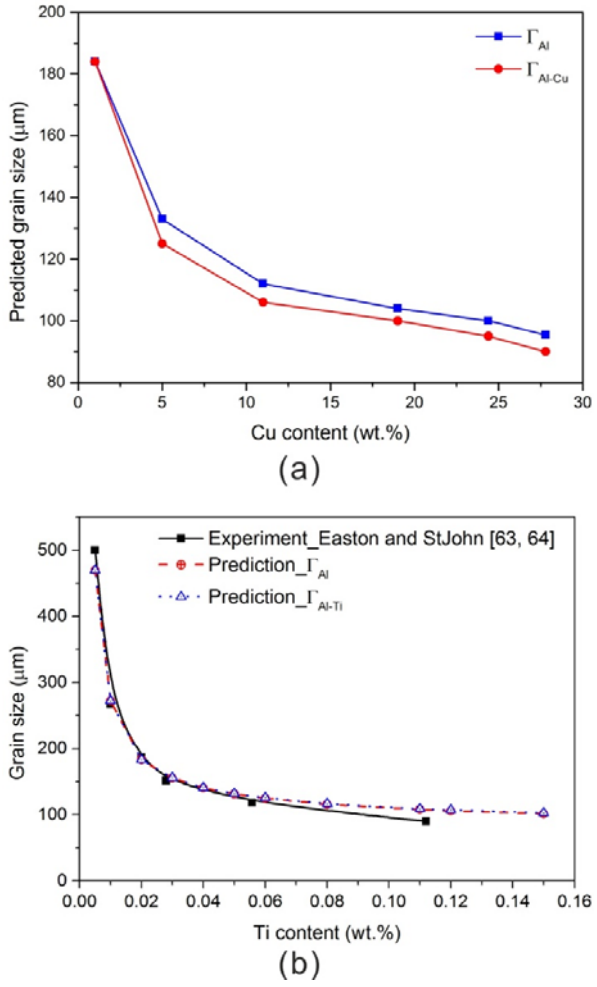

Fig. 7. (a) Predicted grain size of 0.1 wt.% Al-5Ti-1B inoculated Al-Cu alloy as a function of Cu content during isothermal melt solidification under a constant cooling rate of 1 K/s. (b) Predicted and measured [63, 64] grain size of 0.03% TiB2 inoculated Al-Ti alloy as a function of Ti content solidified under an initial cooling rate of 0.8 K/s. The model prediction used composition dependent Gibbs-Thomson coefficient $\Gamma_{Al\text{-}x}$ and the Gibbs-Thomson coefficient of pure Al, Γ_{Al}.

3.2.4. Comparing to the experimental data of Γ

It is difficult to precisely determine the Γ value by experimental methods. The available experimental data of Gibbs-Thomson coefficient Γ for Al alloys were mostly measured by the grain boundary groove method [80]. While for pure Al, Γ was determined indirectly by measuring the solid-liquid interfacial energy using homogeneous nucleation theory [81] or dihedral angle approach [82]. If the maximum value of σ_{SL} (188 mJ/m^2 [83]) measured by experiment is used for estimating the Gibbs-Thomson coefficient Γ for pure Al, it can be obtained that $\Gamma_{Al} = 1.71\ K \cdot m$. Based using the grain boundary groove method [84], it was determined that $\Gamma_{Al-17.3at.\%Cu} = 2.41\ K \cdot m$, $\Gamma_{Al-12.1at.\%Si} = 1.96\ K \cdot m$, $\Gamma_{Al-37.4at.\%Mg} = 1.30\ K \cdot m$ and $\Gamma_{Al-0.0169at.\%Ti} = 1.31\ K \cdot m$, showing $\Gamma_{Al-17.3at.\%Cu}$ and $\Gamma_{Al-12.1at.\%Si}$ are larger than $\Gamma_{Al-37.4at.\%Mg}$ and $\Gamma_{Al-0.0169at.\%Ti}$. This is not consistent with our calculation results. Pompe and Rettenmayr [85, 86] analyzed the influence of quenching rate on the microstructure change, and found out that a cooling rate of larger than 80 K/s is needed for a grain boundary groove analysis of Al-Cu alloys. Hence, as discussed by Lippmann and Rettenmayr [52], the shape of the grain boundary grooves would be influenced by the limited cooling rates by using the radial heat flow apparatus [80]. Another limitation for the grain boundary groove method [52] is that segregation will happen during long time holding which is required for the grain boundary groove experiments. Such a segregation was observed by Bulla et al. [87], which would influence the measured σ_{SL} and therefore the Gibbs-Thompson coefficient. All these reasons may lead to different results between predicted and experimental values. In reality, if the values of entropy of fusion for Al alloys are calculated by the regular solution model or present CALPHAD approach, rather than the ideal solution model used in the grain boundary groove method [84], the calculated σ_{SL} will be much larger than those experimentally measured [88] or calculated by molecular dynamics [89].

4. Conclusions

The influences of solute contents in aluminum alloy on the nucleation driving force (Gibbs free energy change for formation of per unit volume of solid ΔG_v) at a specific undercooling, solid-liquid interfacial energy σ_{SL}, entropy of fusion ΔS_v have been quantitatively investigated. Both eutectic and peritectic forming elements have been evaluated. The critical nucleation activation energy or nucleation barrier of a series of binary alloys was obtained based on the classical heterogeneous nucleation theory. Also, the composition dependent Gibbs-Thomson coefficient Γ was calculated. The conclusions are summarized as follows:

1. The nucleation driving force ΔG_v for Al-Cu and Al-Si is always larger than that for pure Al and increases with increasing solute content for a given undercooling. However, adding Mg will decrease the nucleation driving force. For the three peritectic forming elements below peritectic composition, Ti can increase the nucleation driving force; However, Zr and V both reduce the nucleation driving force.
2. The solid-liquid interfacial energy of aluminum alloys decreases with increasing Cu and Mg solute contents, but increases with Si contents. All of the three peritectic forming elements, Ti, Zr and V, increase the value of σ_{sl} slightly.
3. Based on the classical nucleation theory, adding Si to pure Al increases the nucleation barrier of heterogeneous nucleation and thus reduce the nucleation rate significantly, which could well explain the grain size of un-inoculated Al-Si alloys increases with Si contents at higher Si concentrations reported in the literature.
4. Adding Cu or Mg to pure Al promotes heterogeneous nucleation of aluminum grains. Together with growth restriction and constitutional undercooling effect, Cu and Mg are shown to have the influence of promoting the grain refinement.

5. Three peritectic forming elements Ti, Zr, V have the influence of slightly increasing the nucleation barrier and may reduce the heterogeneous nucleation rate. However, due to the strong growth restriction effect, these solutes will still facilitate nucleation.
6. For solidification of Al alloys inoculated with high potency grain refiner particles, it is revealed that addition of eutectic-forming solute elements can reduce the Γ and thus free growth undercooling ΔT_{fg}, but peritectic-forming solute elements almost have no influence on the Γ and ΔT_{fg}.

Acknowledgments

This research work has been supported by a KPN Project, PRIMAL (project number: 236675), in Norway. The financial support by The Research Council of Norway and the industrial partners, Hydro Aluminum AS, Alcoa Norway AS, is gratefully acknowledged.

References

1. W.L. Fink, K.R. Van Horn and P.M. Budge: *Trans. AIME,* 1931, vol. 93, pp. 421.
2. A. Cibula: *J. Inst. Met.,* 1949-50, vol. 76, pp. 321-60.
3. W. C. Winegard and B. Chalmers: *Trans. ASM,* 1954, vol. 46, pp. 1214-1224.
4. L. A. Tarshis, J. L. Walker and J. W. Rutter: *Metall. Trans.,* 1971, vol. 2, pp. 2589-2597.
5. R. D. Doherty, P. D. Cooper, M. H. Bradbury and F. J. Honey: *Metall. Trans. A,* 1977, vol. 8, pp. 397-402.
6. J. A. Spittle and S. Sadli: *Mater. Sci. Technol.*, 1995, vol. 11, pp. 533-537.
7. W. A. Tiller, K. A. Jackson, J. W. Rutter and B. Chalmers: *Acta Metall.,* 1953, vol. 1, pp. 428-437.
8. H. Xu, L. D. Xu, S. J. Zhang and Q. Han: *Scr. Mater.,* 2006, vol. 54, pp. 2191-2196.
9. J. E. C. Hutt, A. K. Dahle, Y. C. Lee and D. H. StJohn: in *Light Metals 1999,* ed. C. Edmard Eckert, The Minerals, Metals and Materials Soc, Warrendale, 1999, pp.685-692.
10. P Hoefs, W Reif and W Schneider: *Giesserei,* 1994, vol. 81, pp. 398-406.
11. P.A. Tondel: *Grain Refinement of Hypoeutectic Al-Si Foundry Alloys*, in Department of Metallurgy, 1994, Norwegian Institute of Technology, Trondheim, Norway.
12. J. E. C. Hutt, D. H. StJohn, L. Hogan and A. K. Dahle: *Mater.Sci. Technol.*, 1999, vol. 15, pp. 495-500.
13. Y. C. Lee, A. K. Dahle, D. H. StJohn and J. E. C. Hutt: *Mater. Sci. Eng. A*, 1999, vol. 259, pp. 43-52.
14. Z. Chen, H. Kang, G. Fan, J. Li, Y. Lu, J. Jie, Y. Zhang, T. Li, X. Jian and T. Wang: *Acta Mater.,* 2016, vol. 120, pp. 168-178.
15. M. Johnsson and L. Backerud: *Z. Metallk.,* 1996, vol. 87, pp. 216-220.
16. J. Moriceau: *Review of Aluminium,* 1972, vol. 12, pp. 977-988.
17. I. Maxwell and A. Hellawell: *Acta Metall.,* 1975, vol. 23, pp. 229-237.
18. M. Johnsson: *A Critical Survey of the Grain Refining Mechanisms of Aluminium*, 1993, Stockholm University.
19. M. Johnsson: *Thermochim. Acta,* 1995, vol. 256, pp. 107-121.
20. J. D. Hunt: *Mater. Sci. Eng.,* 1984, vol. 65, pp. 75-83.
21. M. Rappaz and P. H. Thévoz: *Acta Metall.,* 1987, vol. 35, pp. 1487-1497.
22. M. Easton and D. StJohn: *Metall. Mater. Trans. A,* 1999, vol. 30, pp. 1613-1623.
23. A. L. Greer, A. M. Bunn, A. Tronche, P. V. Evans and D. J. Bristow: *Acta Mater.,* 2000, vol. 48, pp. 2823-2835.

24. G. Chai, L. Bäckerud and L. Arnberg: *Mater. Sci. Technol.,* 1995, vol. 11, pp. 1099-1103.
25. G. Chai, L. Bäckerud, T. Rølland and L. Arnberg: *Metall. Mater. Trans. A,* 1995, vol. 26, pp. 965-970.
26. W. V. Youdelis: *Metal Sci.,* 1975, vol. 9, pp. 464-466.
27. C.-S. Yang: *Role of nucleation entropy in grain refinement of aluminum alloys*, in Department of *Electrical and Computer Engineering*, 1980, University of Windsor, Canada.
28. W. V. Youdelis and C. S. Yang: *Aluminium,* 1980, pp. 411-413.
29. X. Yao, A. K. Dahle, C. J. Davidson and D. H. StJohn: *J. Mater. Res.,* 2006, vol. 21, pp. 2470-2479.
30. F. Wang, Z.-L. Liu, D. Qiu, J.A. Taylor, M. Easton and M.-X. Zhang: *Metall. Mater. Trans. A,* 2015, vol. 46, pp. 505-515.
31. Q. Du, Y.J. Li: *Acta Mater.,* 2014, vol. 71, pp. 380-389.
32. S.-M. Liang, R. Schmid-Fetzer: *Acta Mater.,* 2014, vol. 72, pp. 41-56.
33. C. Zhang, Y. Du: *Metall. Mater. Trans. A,* 2017, vol. 48A, pp. 5766-5770.
34. T. Keller, G. Lindwall, S. Ghosh, L. Ma, B.M. Lane, F. Zhang, U.R. Kattner, E.A. Lass, J.C. Heigel, Y. Idell, M.E. Williams, A.J. Allen, J.E. Guyer, L.E. Levine: *Acta Mater.,* 2017, vol. 139, pp. 244-253.
35. D. Bardel, M. Perez, D. Nelias, A. Deschamps, C.R. Hutchinson, D. Maisonnette, T. Chaise, J. Garnier, F. Bourlier: *Acta Mater.,* 2014, vol. 62, pp. 129-140.
36. H. Zhang, Y. Wang, S.L. Shang, C. Ravi, C. Wolverton, L.Q. Chen, Z.K. Liu: *Calphad,* 2010, vol. 34, pp. 20-25.
37. A.A. Luo: *Calphad,* 2015, vol. 50, pp. 6-22.
38. R. Schmid-Fetzer, A. Kozlov: *Acta Mater.,* 2011, vol. 59, pp. 6133-6144.
39. J. Eiken, M. Apel, S.-M. Liang, R. Schmid-Fetzer: *Acta Mater.,* 2015, vol. 98, pp. 152-163.
40. A. Malik, J. Odqvist, L. Höglund, S. Hertzman, J. Ågren: *Metall. Mater. Trans. A,* 2017, vol. 48, pp. 4914-4928.
41. Q. Chen, K. Wu, G. Sterner, P. Mason: *J. Mater. Eng. Perform.,* 2014, vol. 23, pp. 4193-4196.
42. W. Cao, F. Zhang, S.-L. Chen, C. Zhang, J. Zhu, S.L. Semiatin, J.S. Tiley: *J. Phase Equilib. Diff.,* 2014, vol. 71, pp. 380-389.
43. J.A. Dantzig and M. Rappaz: *Solidification*,1st ed., EFPL Press, 2009, pp. 264-265.
44. C. V. Thompson and F. Spaepen: *Acta Metall.,* 1983, vol. 31, pp. 2021-2027.
45. J. W. Christian: In *The Theory of Transformations in Metals and Alloys*, 2nd ed., Pergamon, Oxford, 2002, pp. 623-701.
46. I. Ansara, A.T. Dinsdale and M.H. Rand: *COST 507: Thermochemical Database for Light Metal Alloys*, European Communities, Belgium, 1998.
47. A. T. Dinsdale: *Calphad,* 1991, vol. 15, pp. 317-425.
48. J. Li, J. Wang and G. Yang: *J. Cryst. Growth,* 2007, vol. 309, pp. 65-69.
49. D. Huang, S. Liu, Y. Du and B. Sundman: *Calphad,* 2015, vol. 51, pp. 261-271.
50. X.-G. Lu, M. Selleby and B. Sundman: *Calphad,* 2005, vol. 29, pp. 68-89.
51. L. Gránásy and M. Tegze: *Mater. Sci. Forum*, 1991, vol. 77, pp 243-256;
52. S. Lippmann, I.-H. Jung, M. Paliwal and M. Rettenmayr: *Philos. Mag.,* 2016, vol. 96, pp. 1-14.
53. L. Gránásy, M. Tegze and A. Ludwig: *Mater. Sci. Eng. A,* 1991, vol. 133, pp. 577-580.
54. https://www.thermocalc.com
55. https://se.mathworks.com/products/matlab.html

554 56. X. Yao, A. Dahle, C. Davidson, D. StJohn: *J. Mater. Sci.,* 2007, vol. 42, pp. 9756-
555 9764.
556 57. C. W. Bale, E. Bélisle, P. Chartrand, S. A. Decterov, G. Eriksson, K. Hack, I. H. Jung,
557 Y. B. Kang, J. Melançon, A. D. Pelton, C. Robelin and S. Petersen: *Calphad,* 2009, vol. 33,
558 pp. 295-311.
559 58. Y. Yang, B. Song, Z. Yang, G. Song, Z. Cai and Z. Guo: *Mater.,* 2016, vol. 9, pp.
560 1001.
561 59. Y. Birol: *Mater. Sci. Technol.,* 2012, vol. 28, pp. 924-927.
562 60. J. A. Spittle: *Inter. Mater. Rev.,* 2006, vol. 51, pp. 247-269.
563 61. F. Wang, Z. Liu, D. Qiu, J.A. Taylor, M. A. Easton and M.-X. Zhang: *Acta Mater.,*
564 2013, vol. 61, pp. 360-370.
565 62. M.M. Guzowski, G.K. Sigworth, D.A. Sentner: *Metall. Mater. Trans. A,* 1987, vol.
566 18, pp. 603-619.
567 63. Z.W. Chen, M. Easton, D. StJohn: *Metall. Mater. Trans. A,* 1999, vol. 30, pp. 1625-
568 1633.
569 64. M.A. Easton, D.H. StJohn: *Acta Mater.,* 2001, vol. 49, pp. 1867-1878.
570 65. Z.W. Chen, Quasicrystal-enhanced grain refinement and solidification texture
571 envolution in aluminium melts, ICAA15, 2016, Chongqing, China.
572 66. Z.W. Chen, Grain Refinement and Solidification Texture Evolution in Aluminium
573 Alloys, Solidification processing 2017, 2017, Beaumont Estate, Old Windsor, UK.
574 67. G. Kurtuldu, P. Jarry, M. Rappaz: *Acta Mater.,* 2013, vol 61, pp7098-7108.
575 68. G. Kurtuldu, A. Sicco, M. Rappaz: *Acta Mater.,* 2014, vol. 70, pp. 240-248.
576 69. A. L. Greer and T. E. Quested: *Philos. Mag.,* 2006, vol. 86, pp. 3665-3680.
577 70. A. L. Greer, T. E. Quested and J. E. Spalding: In *Light Metals 2002*, ed. W.A.
578 Schneider, The Minerals, Metals and Materials Society, Warrendale, 2002, pp 687-694;
579 71. T. E. Quested and A. L. Greer: *Acta Mater*., 2004, vol. 52, pp. 3859-3868.
580 72. T. E. Quested and A. L. Greer: Acta Mater., 2005, vol. 53, pp. 4643-4653.
581 73. D. Shu, B. Sun, J. Mi and P. S. Grant: *Acta Mater*., 2011, vol. 59, pp. 2135-2144.
582 74. Q. Du and Y. J. Li: *Acta Mater*., 2014, vol. 71, pp. 380-389.
583 75. Q. Du and Y. J. Li: *Mater. Sci. Forum*, 2014, vol. 790-791, pp. 185-190.
584 76. Q. Du and Y. J. Li: IOP Conference Series: Mater. Sci. Eng., 2015, vol. 84,
585 pp.012015.
586 77. Y. Xu, Q. Du and Y. Li: *Trans. Indian Inst. Met*., 2015, vol. 68, pp. 1013-1016.
587 78. M.A. Martorano, D.T. Aguiar and J.M.R. Arango: *Metall. Mater. Trans. A,* 2015, vol.
588 46, pp. 377-395.
589 79. Y. Xu, D. Casari, Q. Du, R.H. Mathiesen, L. Arnberg and Y. Li: *Acta Mater.,* 2017, In
590 Press, doi: 10.1016/j.actamat.2017.08.053.
591 80. M. Gündüz and J. D. Hunt: *Acta Metall.,* 1985, vol. 33, pp. 1651-1672.
592 81. D. Turnbull: *J. Appl. Phys.,* 1950, vol. 21, pp. 1022-1028.
593 82. M. E. Glicksman and C. L. Vold: *Acta Metall.,* 1969, vol. 17, pp. 1-11.
594 83. D. Camel, N. Eustathopoulos and P. Desré, *Acta Metall.,* 1980, vol. 28, pp. 239-247.
595 84. Y. Altıntas, S. Aksöz, K. Keşlioğlu and N. Maraşlı: *J. Alloys Compd.,* 2015, vol. 649,
596 pp. 453-460.
597 85. O. Pompe and M. Rettenmayr: *Pract. Metallogr.,* 1998, vol. 35, pp. 203-211.
598 86. O. Pompe and M. Rettenmayr: *J. Cryst. Growth,* 1998, vol. 192, pp. 300-306.
599 87. A. Bulla, C. Carreno-Bodensiek, B. Pustal, R. Berger, A. Bührig-Polaczek and A.
600 Ludwig: *Metall. Mater. Trans. A,* 2007, vol. 38, pp. 1956-1964.
601 88. H. Jones: *Metall. Mater. Trans. A,* 2007, vol. 38, pp. 1563-1569.
602 89. L. Wu, B. Xu, Q. Li, W. Liu and M. Li: *J. Mater. Res.,* 2015, vol. 30, pp. 1827-1835.

List of Figure Captions

Fig. 1. Schematic mole Gibbs free energy-composition diagram: (a) at the liquidus temperature, T_L, (b) below T_L, at arbitrary nucleation temperature. The free energy change ΔG associated with forming a small nucleus of composition c_S in the liquid of composition c_L is obtained by the parallel tangent construction [44,45]. Adapted from [44] with additional data from [45].

Fig. 2. Calculated Gibbs free energy change per undercooling $\Delta G_v/\Delta T$, solid-liquid interfacial energy σ_{SL}, relative critical nucleation energy and relative Ψ to pure Al, $\frac{\Delta G^0_{n,Al-X}}{\Delta G^0_{n,Al}}$ and $\frac{\Psi_{Al-X}}{\Psi_{Al}}$, with different solute contents (at.%) at three different undercoolings $\Delta T = 1, 5, 10\ K$ for hypoeutectic Al-Cu alloys.

Fig. 3. Calculated Gibbs free energy change ΔG_v, solid-liquid interfacial energy σ_{SL}, relative critical nucleation energy and relative Ψ to pure Al, $\frac{\Delta G^0_{n,Al-X}}{\Delta G^0_{n,Al}}$ and $\frac{\Psi_{Al-X}}{\Psi_{Al}}$, with different solute contents (at.%) at undercooling $\Delta T = 1\ K$ for hypoeutectic Al-Cu, Al-Mg and Al-Si alloys.

Fig. 4. Calculated Gibbs free energy change ΔG_v, solid-liquid interfacial energy σ_{SL}, relative critical nucleation energy and relative Ψ to pure Al, $\frac{\Delta G^0_{n,Al-X}}{\Delta G^0_{n,Al}}$ and $\frac{\Psi_{Al-X}}{\Psi_{Al}}$, with different solute contents (at.%) at undercooling $\Delta T = 1\ K$ for hypoperitectic Al-Ti, Al-Zr and Al-V alloys.

Fig. 5. Calculated entropy of fusion per unit volume ΔS_v, and relative Gibbs-Thompson coefficient Γ to pure Al, $\frac{\Gamma_{Al-X}}{\Gamma_{Al}}$, with different solute contents (at.%) at respective liquidus temperature for hypoeutectic Al-Cu, Al-Mg and Al-Si alloys.

Fig. 6. Calculated entropy of fusion per unit volume ΔS_v, and relative Gibbs-Thompson coefficient Γ to pure Al, $\frac{\Gamma_{Al-X}}{\Gamma_{Al}}$, with different solute contents (at.%) at respective liquidus temperature for hypoperitectic Al-Ti, Al-Zr and Al-V alloys.

Fig. 7. (a) Predicted grain size of 0.1 wt.% Al-5Ti-1B inoculated Al-Cu alloy as a function of Cu content during isothermal melt solidification under a constant cooling rate of 1 K/s. (b) Predicted and measured [63, 64] grain size of 0.03% TiB2 inoculated Al-Ti alloy as a function of Ti content solidified under an initial cooling rate of 0.8 K/s. The model prediction used composition dependent Gibbs-Thomson coefficient $\Gamma_{Al\text{-}x}$ and the Gibbs-Thomson coefficient of pure Al, Γ_{Al}.